Comparison of sand liquefaction in cyclic triaxial and simple shear tests

Article *in* SOILS AND FOUNDATIONS · June 2021

DOI: 10.1016/j.sandf.2021.05.002

3 authors:

Zhenzhen Nong
Jiangsu University of Science and Technology
9 PUBLICATIONS **16** CITATIONS
SEE PROFILE

Sung-Sik Park
Kyungpook National University
95 PUBLICATIONS **919** CITATIONS
SEE PROFILE

dong-eun Lee
Kyungpook National University
155 PUBLICATIONS **1,061** CITATIONS
SEE PROFILE

HOSTED BY

ELSEVIER

Available online at www.sciencedirect.com

ScienceDirect

Soils and Foundations xxx (xxxx) xxx

SOILS AND FOUNDATIONS

www.elsevier.com/locate/sandf

Technical Paper

Comparison of sand liquefaction in cyclic triaxial and simple shear tests

Zhen-Zhen Nong [a], Sung-Sik Park [b,*], Dong-Eun Lee [c]

[a] School of Naval Architecture and Ocean Engineering, Jiangsu University of Science and Technology, Zhenjiang, China
[b] Department of Civil Engineering, Kyungpook National University, 1370, Sangyeok-dong, Buk-gu, Daegu 702-701, Republic of Korea
[c] Department of Architectural Engineering, Kyungpook National University, 1370, Sangyeok-dong, Buk-gu, Daegu 702-701, Republic of Korea

Received 1 September 2020; received in revised form 1 May 2021; accepted 13 May 2021

Abstract

The liquefaction resistance and correction factors K_σ and K_α of Nakdong River sand obtained from cyclic triaxial (CTX) tests were compared with those determined by cyclic simple shear (CSS) tests to ascertain the importance of the reduction factor C_r and correction factors K_σ and K_α in liquefaction evaluations, especially in view of the lack of comparative liquefaction assessments based on different laboratory test apparatuses. All samples used for the comparisons were obtained from the same type of sand by using similar preparation methods and they were subjected to similar stress states to minimize the number of factors influencing the comparison results; moreover, the apparatuses used in the two tests were manufactured by the same company and all tests were conducted by a single operator. It was found that the liquefaction resistance in CTX tests was always greater than that in CSS tests. Furthermore, C_r varied from 0.63 to 0.36, and it depended on the relative density D_r and initial static shear ratio α. K_σ, which increased with the normal effective stress σ'_{nc} in CTX tests, was identical to K_σ observed in CSS tests when α was increased up to 0.1. By contrast, K_α in the CSS tests was 58%–97% of K_α measured in the CTX tests, and it depended on the combined effect of D_r, σ'_{nc}, and α. The relationship between K_α and α in both CTX and CSS tests was well represented by a parabolic function. Moreover, the differences in K_α values between the CTX and CSS tests were also found to be a parabolic function of α. This information can be used for converting CTX (or CSS) values into equivalent CSS (or CTX) values.

Keywords: Sand liquefaction; Cyclic triaxial test; Cyclic simple shear test

1. Introduction

Cyclic triaxial (CTX) and cyclic simple shear (CSS) tests are useful tools that are very commonly used in laboratories for evaluating the liquefaction behavior of soils. However, for given test conditions, each of them yields a different liquefaction resistance since their capability to simulate the cyclic stress states resulting from earthquakes depends on the nonuniformity of stresses and strains in the sample, the rotation of the principal axis, the duplication of the plane strain condition, and the specifics of the stress conditions imposed (Bhatia et al. 1985). Previous comparative studies have indicated that CTX tests predict a higher liquefaction resistance compared with CSS tests. C_r, which is among the CTX parameters used to observe the responses of samples under CSS conditions, has been studied within a limited scope (Peacock and Seed 1968). Vaid and Sivathayalan (1996) found that C_r is dependent on both the relative density D_r and confining stress level: for loose sand (D_r = 31%–40%), C_r was about 0.78 irrespective

Peer review under responsibility of The Japanese Geotechnical Society.
* Corresponding author.
E-mail addresses: zznong@foxmail.com (Z.-Z. Nong), sungpark@knu.ac.kr (S.-S. Park), dolee@knu.ac.kr (D.-E. Lee).

https://doi.org/10.1016/j.sandf.2021.05.002
0038-0806/

Please cite this article as: Z.-Z. Nong, S. S. Park and D. E. Lee, Comparison of sand liquefaction in cyclic triaxial and simple shear tests, Soils and Foundations, https://doi.org/10.1016/j.sandf.2021.05.002

of the confining stress, and for dense sand (D_r = 59%–72%), C_r increased from about 0.62 to about 0.7 when the confining stress increased from 50 to 400 kPa. Hoque (2016) observed C_r-values of 0.55, 0.61, and 0.7 for loose (D_r = 40%), medium (D_r = 60%), and dense (D_r = 80%) sand, respectively. In practice, a C_r-value of 0.6 is adopted without regard to the confining stress and relative density. Sivathayalan and Ha (2011) suggested that the effect of the initial static shear stress should not be ignored when calculating the C_r-value. However, no study has investigated how the initial static shear stress influences C_r. The C_r-values obtained by different researchers are inconsistent, and more research is required to consider the discrepancy in the cyclic resistance between the CSS and CTX tests, especially for soil elements subjected to an initial static shear stress.

It is generally acknowledged that the liquefaction resistance of sand decreases with increasing vertical effective stress (e.g., Marcuson and Krinitzsky 1976; Seed and Idriss 1981; Seed and Harder 1990; Harder and Boulanger 1997; Sze 2010). A correction factor, K_σ, has been widely used in studies when the influence of the vertical effective stress, in both the CTX and CSS tests. Nonetheless, K_σ-values in CTX tests have rarely been compared with those in CSS tests. Vaid and Sivathayalan (1996) compared K_σ-values in CSS tests with those obtained by Vaid and Thomas (1995) in CTX tests. For loose sand, the K_σ-values of both tests were nearly identical, whereas for dense sand, the K_σ-values in the CTX tests appeared to have been overestimated when compared with those in the CSS tests. Since field conditions are closer to CSS test conditions, adopting K_σ-values measured by CTX tests would lead to further conservatism in designs for dense sand (Vaid and Sivathayalan 1996; Vaid et al. 2001; Boulanger 2003). Fonseca et al. (2015) suggested that investigations of K_σ should not consider only the effect of initial confining stress, but recognize the potential influence of the fabric induced by the rotation of principal stresses, such as can be better investigated in a CSS apparatus than a CTX apparatus. For critical projects, the National Center for Earthquake Engineering Research (NCEER) (Youd et al. 2001) recommends the use of site-specific K_σ-values. Since different laboratory test methods yield different amplitudes of K_σ, additional research is required to reduce the difference in the amplitudes.

It is desirable to compare the liquefaction resistance determined from CTX and CSS tests for sand subjected to an initial static shear stress. The value of another correction factor, K_α, accounts for the presence of an initial static shear stress at a given relative density, and it can differ drastically between test methods (Sivathayalan and Ha 2011). Hosono and Yoshimine (2004) found that the values of K_α for CSS conditions were 75%–85% of those evaluated by CTX tests in the presence of an initial compression static shear stress when the initial static shear ratio (α) range between 0.2 and 0.4. Sze (2010) compiled data from Vaid et al. (2001) and Wijewickreme et al. (2005) and compared the relationship between K_α and α on the basis of results obtained from the CTX and CSS tests. For loose sand (D_r = 40%), an increase in α resulted in an increasing trend in the K_α-value for CTX tests; however, an increase in α resulted in the opposite trend for CSS tests. Owing to the limited number of studies on this topic, existing understanding of K_σ and K_α in CTX and CSS tests is inadequate, and therefore, further investigations are required.

In view of the importance of C_r, K_σ, and K_α in liquefaction evaluations and the lack of comparative liquefaction assessments based on different laboratory testing apparatuses, a comprehensive experimental study of CTX and CSS tests was conducted using Nakdong River sand. The main objectives of this study were to i) compare CTX liquefaction resistances with those obtained under CSS conditions to determine the effect of the initial static shear stress on C_r, ii) determine the effect of the initial static shear stress on K_σ in both the CTX and CSS tests and to compare K_σ values obtained in an experiment with the predictions of existing empirical methods to assess the appropriateness of K_σ determination in practice; and iii) relate K_α obtained in the CTX and CSS tests and to make an attempt to provide a convenient method of conversion of CSS K_α into CTX K_α and vice versa. Furthermore, comparisons between the two tests were made by considering samples of the same type of sand, using similar methods of sample preparation, similar relative densities, and similar stress states to minimize the number of factors influencing the comparison results; moreover, the apparatuses used in both tests were manufactured by a single company and both tests were conducted by a single operator.

2. Experimental program

2.1. Stress states in the CTX and CSS tests

The stress state in the CTX test is significantly different from that in the CSS test. In the CTX test, soil specimens can be consolidated under isotropic or anisotropic conditions to simulate a soil element under in-ground conditions. As shown in Fig. 1(a), for isotropic consolidation, the confining stress (σ'_c) applied to the specimen in the vertical and horizontal directions are equal. Earthquake loading is simulated by applying a cyclic deviator stress (q_{cyc}) by simultaneously increasing the confining stress in the vertical direction and decreasing the confining stress in the horizontal direction by an equal amount; the application of q_{cyc} is accompanied by the instantaneous rotation of principal stress directions by 90°. In this process, a constant normal effective stress (σ'_{nc}) is applied to the specimen in the 45° plane, and the direction of shear stress (τ_{cyc}) in this 45° plane is reversed when the above-mentioned vertical and horizontal stresses are reversed. The conditions in the 45° plane (or the plane of maximum shear stress) are representative of the stress state in the horizontal plane for in situ conditions. The cyclic stress ratio (CSR), normal effective

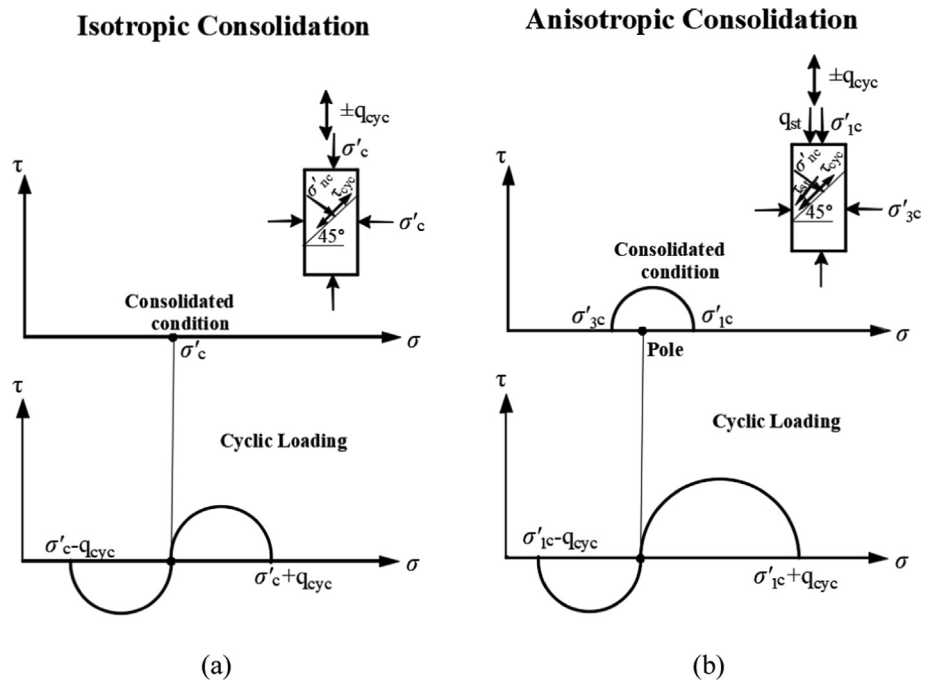

Fig. 1. Stress conditions in CTX test.

stress (σ'_{nc}), and shear stress (τ_{cyc}) in the 45° plane in the CTX test are defined as

$$CSR = \frac{q_{cyc}}{\sigma'_{1c} + \sigma'_{3c}} = \frac{\tau_{cyc}}{\sigma'_{nc}}; \sigma'_{nc} = \frac{\sigma'_{1c} + \sigma'_{3c}}{2}; \tau_{cyc} = \frac{q_{cyc}}{2} \quad (1)$$

For anisotropic consolidation, as shown in Fig. 1(b), the major principal stress (σ'_{1c}) is different from the minor principal stress (σ'_{3c}), and this results in an initial deviator stress (q_{st}) in the vertical direction and an initial static shear stress (τ_{st}) in the 45° plane. The initial static shear ratio (α) in the 45° plane is defined as

$$\alpha = \frac{q_{st}}{2\sigma'_{nc}} = \frac{\tau_{st}}{\sigma'_{nc}} = \frac{\sigma'_{1c} - \sigma'_{3c}}{\sigma'_{1c} + \sigma'_{3c}} \quad (2)$$

The stress state in the CSS test is closer to in situ conditions compared with that in the CTX test. Furthermore, in the CSS test, the stress conditions in the horizontal plane (or the plane of maximum shear stress) can be considered to be identical to those at the in situ soil surface. As shown in Fig. 2, the soil element is consolidated under the K_0 condition. A vertical effective stress (σ'_{v0}) is applied to the horizontal plane and the horizontal deformation is constrained by a wire-reinforced membrane or Teflon-coated stacked aluminum rings. Additionally, a cyclic shear stress (τ_{cyc}) is applied to the horizontal plane to simulate the vertically propagating shear wave generated by earthquake loading. The CSR in the CSS test is defined as

$$CSR = \frac{\tau_{cyc}}{\sigma'_{v0}} \quad (3)$$

Moreover, an initial static shear stress (τ_{st}) is introduced in the horizontal direction during the consolidation phase. The initial static shear ratio (α) in the representative plane, is defined as

$$\alpha = \frac{\tau_{st}}{\sigma'_{v0}} \quad (4)$$

Despite the debate on whether laboratory stress conditions match in situ stress conditions in the CTX test, this test is still widely used to evaluate soil liquefaction owing to the availability of the test apparatus and researchers' familiarity with the test procedure and apparatus. On the other hand, while the CSS test is more realistic for representing sand liquefaction behavior under earthquake loading, the complexity of specimen preparation, significant nonuniformity of stresses and strains, and general apparatus unavailability are its major disadvantages.

2.2. Test apparatuses

The apparatuses used for the CTX and CSS tests in this study were manufactured by Geocomp Corporation. The CTX apparatus (Fig. 3a) was controlled by a feed-forward adaptive control system and it could accurately apply and maintain axial loads by using a stepper motor coupled to a low-backlash, low-inertia, and linear electromechanical actuator. The loads were measured using an internal low-profile load cell with a capacity of 4.44 kN and a resolution of 0.5 N. Axial displacements were measured using a displacement transducer attached to the top of the chamber; the transducer had a range and a resolution of 50 mm and 7.5×10^{-4} mm, respectively. Pres-

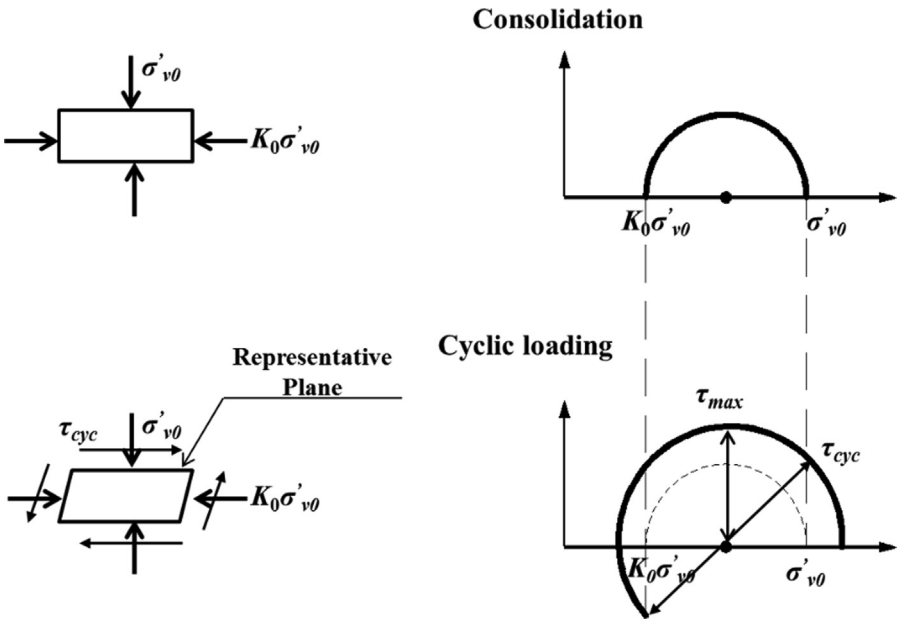

Fig. 2. Stress conditions in CSS test.

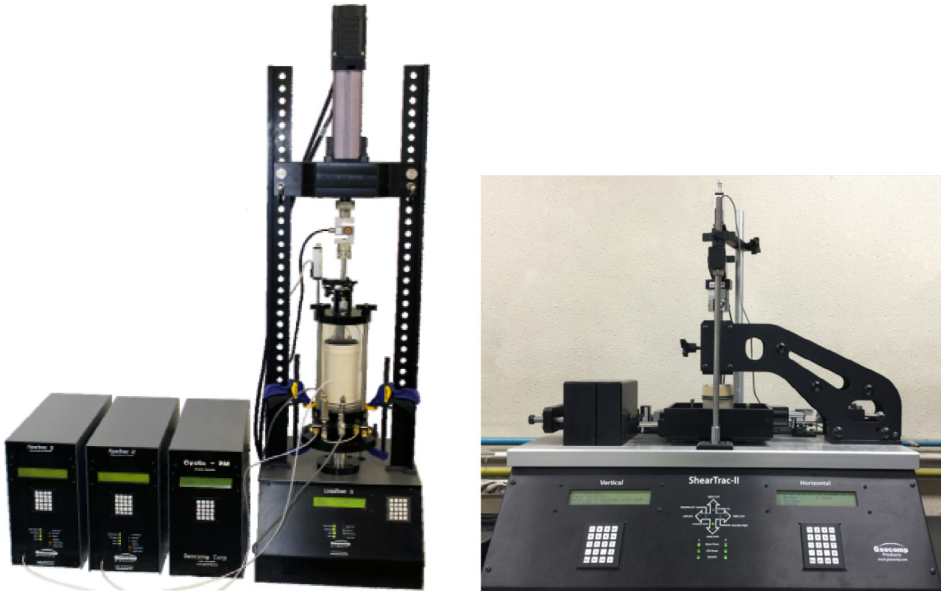

(a) CTX apparatus (b) CSS apparatus

Fig. 3. Test apparatuses used in this study.

sure was applied to the cell and sample by using a dual-loop pneumatic regulator with a capacity of 1,400 kPa and a resolution of 0.06 kPa.

The CSS apparatus (Fig. 3b) was developed by the Norwegian Geotechnical Institute (NGI type; Bjerrum and Landva 1966) and had stepper motors with built-in controls for vertical and horizontal loads and displacements. Both the vertical and horizontal loads were measured using a low-profile load cell with a capacity of 5 kN and a resolution of 0.5 N, and the vertical displacement was measured using a displacement transducer with a range and a resolution of 25.45 mm and 1.3×10^{-3} mm, respectively. Horizontal displacements were measured using a displacement transducer with a range and a resolution of 12.5 mm and 1.3×10^{-3} mm, respectively. In particular, constant volume conditions were maintained through closed-loop computer control, with a vertical displacement sensor providing feedback.

2.3. Test material

The material used in this study was Nakdong River sand, which was collected from banks of the Nakdong River. It was uniform, siliceous, medium, nonplastic sand

comprising quartz particles with angular to subangular shapes and with a specific gravity of 2.64. The minimum and maximum void ratios according to the Japanese standard (JIS A 1224, 2009) were 0.65 and 1.181, respectively. The sand was classified as poorly graded sand (SP) according to the Unified Soil Classification System, and its physical properties are listed in Table 1. A scanning electron microscopy photograph and the grain size distribution curve of the sand are shown in Figs. 4 and 5, respectively. After collection, the sand was washed and dried, and it was subsequently sieved to obtain particle sizes of 0.85 and 0.075 mm.

2.4. Sample preparation and test programs

CTX specimens with an initial size of 142 mm (height) × 71 mm (diameter) were reconstituted using the dry air pluviation technique. All specimens were initially pluviated in the loosest state possible by controlling the funnel opening to maintain the minimal drop height above the sand surface. Specimens with the desired density were obtained by uniformly tapping the periphery of the mold using a rubber hammer. The relative densities of the specimens were determined by calculating the specimen volumes and sand masses. The pore air in the specimen was replaced by carbon dioxide before inundation, and back pressure saturation was performed prior to shear. Sample saturation was achieved by ensuring that the pore pressure parameter B was equal to or greater than 0.95 before the test.

A CSS specimen was laterally confined in a wire-reinforced membrane that prevented the horizontal extension of the specimen. Cylindrical specimens with dimensions of 63.5 mm (diameter) × 25 mm (height) were reconstituted using the dry compaction technique (Ladd 1978). For loose sand ($D_r = 40\%$), the amount of dry sand used each time was identical, and the sand was compacted lightly to achieve the desired height. For dense sand ($D_r = 80\%$), the specimen was separated into five layers, with all layers containing the same amount of sand. The lower layers were compacted to a height slightly greater than 5 mm by trial and error. The relative densities of the specimens were determined from the sand mass and the specimen volume after consolidation. The saturation level of dry sand was ignored in the CSS tests.

The preparation method for the CTX specimens was slightly different from that used for the CSS specimens. The sand fabric was essentially similar because dry sand was initially used for sample preparation both in the CTX and CSS tests. Silver et al. (1980) found that while the sample preparation method significantly influenced the CTX strength, this was not the case for the CSS strength. Therefore, the delicate difference in the sample preparation method used in this study was not considered to be a significant factor in the analysis of the differences in specimen behavior between the CTX and CSS tests.

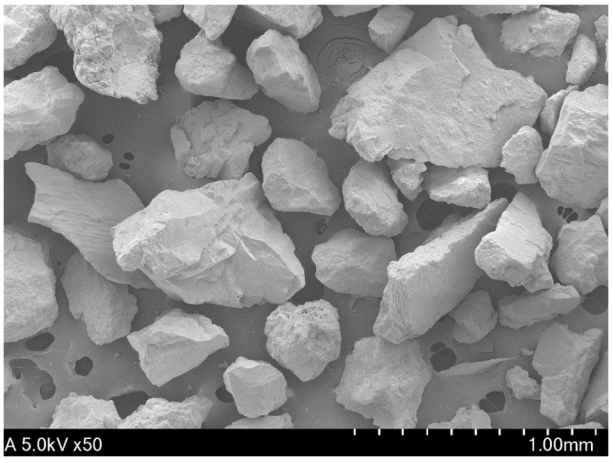

Fig. 4. SEM image of Nakdong river sand.

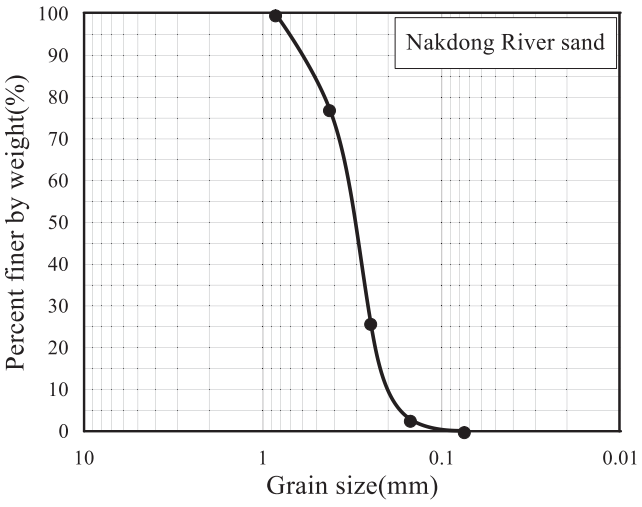

Fig. 5. Grain size distribution curve of Nakdong river sand.

The testing program for the CTX tests is shown in Table 2. Specimens with relative densities of 40% and 80% were prepared, and all specimens were consolidated under both isotropic and anisotropic conditions by applying normal effective stresses of 100 and 200 kPa, respectively. For achieving anisotropic consolidation, a broad range of initial static shear stress ratios, namely, 0.05, 0.1, 0.2, and 0.4, were used for the compressed side. Cyclic

Table 1
Material properties of Nakdong river sand.

Index properties								
Specific gravity	D_{10} (mm)	D_{30} (mm)	D_{60} (mm)	C_u	C_c	e_{max}	e_{min}	USCS
2.64	0.18	0.28	0.37	2.056	1.177	1.181	0.65	SP

Table 2
Testing program for cyclic triaxial tests.

Sample	α	σ'_{nc} (kPa)	σ'_{3c} (kPa)	σ'_{1c} (kPa)	q_{st} (kPa)	p′ (kPa)
Loose (D_r = 40%)	0	100	100	100	0	100
	0.05	100	95	105	10	98.3
	0.1	100	90	110	20	96.7
	0.2	100	80	120	40	93.3
	0.4	100	60	140	80	86.7
	0	200	200	200	0	200
	0.05	200	190	210	20	196.7
	0.1	200	180	220	40	193.3
	0.2	200	160	240	80	186.7
	0.4	200	120	280	160	173.3
Dense (D_r = 80%)	0	100	100	100	0	100
	0.05	100	95	105	10	98.3
	0.1	100	90	110	20	96.7
	0.2	100	80	120	40	93.3
	0.4	100	60	140	80	86.7
	0	200	200	200	0	200
	0.05	200	190	210	20	196.7
	0.1	200	180	220	40	193.3
	0.2	200	160	240	80	186.7
	0.4	200	120	280	160	173.3

Note: p′ is the mean effective normal stress.

loading was applied in a stress-controlled mode under undrained conditions. A loading frequency of 0.1 Hz (reflecting a sinusoidal function) was used for obtaining suitable input and output responses, and the tests were controlled until the specimen deformation reached a level where the specified axial strain level was exceeded.

Table 3 shows the testing program for the CSS tests. The specimens were prepared with relative densities of 40% and 80%. Briefly, dry sand specimens were consolidated under vertical effective stresses of 100, 150, and 200 kPa, and initial static shear stress ratios of 0, 0.05, 0.1, and 0.2 were used for each vertical effective stress level. Cyclic shear loading was applied in a stress-controlled mode at a frequency of 0.1 Hz (reflecting a sinusoidal function). All the specimens were tested under undrained shear conditions by imposing constant volume conditions, and the vertical loads were adjusted using the vertical load frame to maintain a constant volume. Furthermore, the excess pore pressure generated in the cyclic shear phase was equal to the change in the vertical effective stress.

2.5. Liquefaction criteria

The term liquefaction is used herein to refer to all forms of deformation, without regard to the actual strain development mechanism. Liquefaction criteria can be defined on the basis of either the pore pressure ratio or the axial/shear strain. However, a pore-pressure-based liquefaction criterion is not appropriate to define the onset of liquefaction in laboratory tests since 1) it would not be applicable to sand exhibiting the flow failure type of deformation (Sivathayalan and Ha 2011) and 2) the excess pore water pressure ratio in dense sand did not reach 100% of the initial effective confining pressure owing to dilatancy. Consequently, the liquefaction criteria used in this study were based on the axial/shear strain, in accordance with the rec-

Table 3
Testing program for cyclic simple shear tests.

Sample	α	σ'_{v0} (kPa)	τ_{st} (kPa)	Sample	α	σ'_{v0} (kPa)	τ_{st} (kPa)
Loose (D_r = 40%)	0	100	0	Dense (D_r = 80%)	0	100	0
	0.05	100	5		0.05	100	5
	0.1	100	10		0.1	100	10
	0.2	100	20		0.2	100	20
	0	150	0		0	150	0
	0.05	150	7.5		0.05	150	7.5
	0.1	150	15		0.1	150	15
	0.2	150	30		0.2	150	30
	0	200	0		0	200	0
	0.05	200	10		0.05	200	10
	0.1	200	20		0.1	200	20
	0.2	200	40		0.2	200	40

ommendation of the National Research Council (NRC 1985). The criteria have been widely used by many researchers (e.g., Toki et al. 1986; Pillai and Stewart 1994; Ishihara 1996; Vaid and Sivathayalan 1996; Yang and Sze 2011a). CTX specimens with total or partial stress reversals were deemed to undergo liquefaction when the double amplitude (DA) axial strain exceeded 5%. In the case of specimens without stress reversals, the occurrence of a peak axial strain of 5% was considered a valid criterion since strain development was unidirectional. On the other hand, CSS specimens with total or partial stress reversals were deemed to undergo liquefaction when the DA shear strain exceeded 7.5%, and specimens without stress reversals were deemed to undergo liquefaction when the peak shear strain exceeded 7.5%. The onset of liquefaction was also defined for characterizing cyclic responses (Yang and Sze 2011b). Park et al. (2020) studied the cyclic behavior of loose and dense Nakdong River sand in CSS tests, and they observed that sudden shear strain runaway is the main reason for the liquefaction of loose sand, whereas plastic strain accumulation was the principal cause of the liquefaction of dense sand. A careful examination of the cyclic curves for loose Nakdong River sand showed that the number of cycles to liquefaction was consistent, irrespective of whether the onset of liquefaction was defined on the basis of the sudden shear strain runaway or the attainment of a specified shear strain. Thus, the use of a specific strain level to define the liquefaction of both loose and dense sand was unlikely to influence the test results.

The number of cycles to liquefaction is generally defined in the range of 10–20 cycles (e.g., Haeri and Pouragha 2010; Yang and Sze 2011b; Wei and Yang 2015). Liu et al. (2001) indicated that for a magnitude 7.5 earthquake, the equivalent number of uniform stress cycles considered as the median prediction of empirical models is 19 for laboratory tests. Since the number of cycles to liquefaction is only used as a reference and does influence the comparisons and corollary conclusions discussed below, the cyclic resistance ratio (CRR) is defined as the value of CSR in 15 loading cycles and denoted by CRR_{15} in discussions of further analysis. According to Seed et al. (1975), the choice of 15 cycles corresponds to a magnitude 7.5 earthquake.

3. Test results and discussion

A comprehensive CTX and CSS testing program comprising 144 tests was conducted using Nakdong River sand. During both the CTX and CSS tests, for given relative density and stress state, three tests with different cyclic shear stress ratios were conducted to obtain the cyclic resistance curve (number of cycles versus CSR). CSR was appropriately chosen to ensure the occurrence of failure within a significant number of cycles, which facilitated the computation of the liquefaction resistance values. For every combination of σ'_{nc} (or σ'_{v0}), α, and D_r, tests were repeated until the number of cycles to liquefaction in two successive test runs had a relative error below 10%. The CRR values for 15 loading cycles (CRR_{15} in the figures) were obtained from the cyclic resistance curves.

On the basis of the earlier discussion, the magnitude of the normal effective stress in the 45° plane in the CTX tests was considered as an appropriate measure of the initial confinement of the specimens. This was consistent with the CSS test conditions, in which the initial confinement was in the horizontal plane. The following sections discuss the comparison of the liquefaction resistance and correction factors K_σ and K_α between the CTX tests (based on a 45° plane) and the CSS tests (based on a horizontal plane).

3.1. Comparison of liquefaction resistance

Fig. 6 shows a comparison of the variation of the liquefaction resistance with α, as a function of σ'_{nc} (or σ'_{v0}), for CTX and CSS tests. For given D_r and α values, an increase in σ'_{nc} (or σ'_{v0}) resulted in a decrease in the liquefaction resistance in 15 cycles for both types of tests. In particular, the liquefaction resistance in the CTX tests was always greater than that in the CSS tests, regardless of the density state. Clearly, the CRR_{15} behavior during the CTX tests, which was influenced by α, differed considerably from that during the CSS tests. For loose sand, as shown in Fig. 6(a), regardless of how σ'_{nc} (or σ'_{v0}) varied, the value of CRR_{15} in the CTX tests increased from 0.2 to about 0.4 as α increased from 0 to 0.4. By contrast, in the CSS tests, the value of CRR_{15} decreased from about 0.15 to about 0.1 as α increased from 0 to 0.2. The different loading modes of the CTX and CSS tests and particle effects may be responsible for these discrepancies (Wijewickreme et al. 2005). During CTX tests, for a given confining stress, an increase in the initial static shear decreases the cyclic resistance only if the strain development mechanism is strain softening. The cyclic resistance increases if this mechanism is cyclic mobility (Vaid and Chern 1985). Careful examinations of the strain development mechanism have revealed that a relative density of 30% is the upper limit for strain softening to cause liquefaction (Vaid et al. 2001). Notably, for a given σ'_{nc}, the liquefaction resistance of Nakdong River loose sand ($D_r = 40\%$) increased with α in CTX tests. Furthermore, the failure mechanism of loose sand in CTX tests was verified as cyclic mobility in this study. For dense sand, as shown in Fig. 6(b), the CRR_{15} values in CTX tests increased continuously with α and were independent of σ'_{nc}. However, the variations of CRR_{15} with α for dense sand in the CSS tests were dependent on both α and σ'_{v0}. For $\sigma'_{v0} = 100$ kPa, CRR_{15} increased gradually with an increase in α from 0 to 0.2, and for $\sigma'_{v0} = 150$ and 200 kPa, CRR_{15} increased gradually with an increase in α to 0.1 and then slightly decreased when α further increased to 0.2. Tatsuoka et al. (1982) found that for dense sand, the effect of the initial static shear stress on the liquefaction resistance may differ between CTX and CSS tests. They attributed this difference to the difference in the shearing mechanism between the two tests.

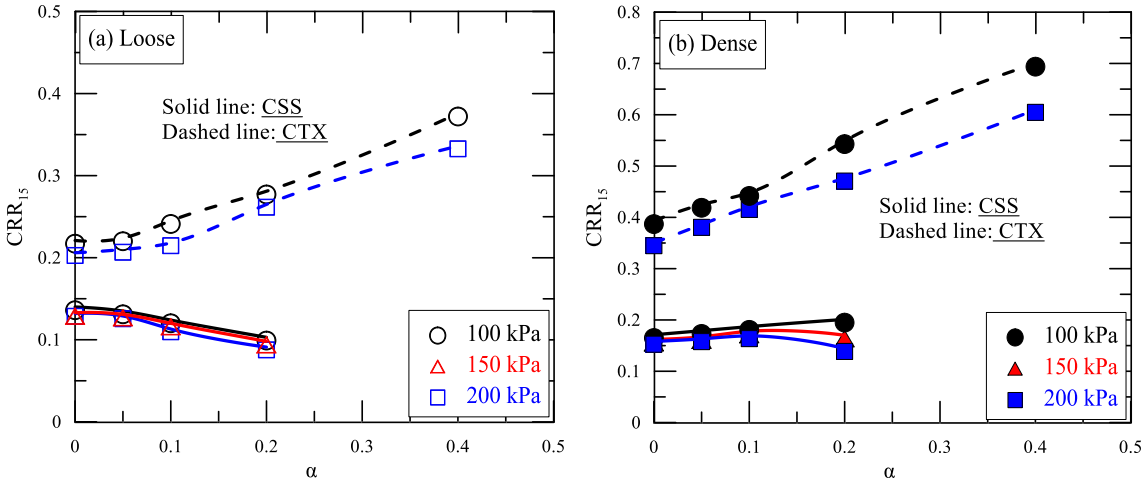

Fig. 6. Comparison of CRR_{15}–α measured in CTX and CSS tests.

A comparison of CRR_{15}–σ'_{nc} (or σ'_{v0}) curves as a function of α for CTX and CSS tests is presented in Fig. 7. All CRR_{15}–σ'_{nc} (or σ'_{v0}) curves for CTX tests (located in the upper portion) again indicate a higher liquefaction resistance compared with those observed for the CSS tests. Compared with CSS tests, the liquefaction resistance increases sharply with an increase in α when α reaches a high level in CTX tests. On the other hand, the relative flattening of the CRR_{15}–σ'_{nc} (or σ'_{v0}) curves in CSS tests indicates that the decrease in CRR_{15} with an increase in σ'_{nc} (or σ'_{v0}) is small, but this decrease becomes significant when the initial static shear stress increases. Zhang and Evans (2018) simulated the behavior of granular assemblies subjected to dynamic loading in both CTX and CSS conditions by using the discrete element method (DEM). They indicated that specimens in CTX and CSS tests behave differently at the microscale; the CTX tests cannot produce pure shear waves, while the CSS tests can. Since the CSS tests closely simulate in situ loading conditions associated with vertically propagating shear waves caused by an earthquake, the liquefaction resistance determined for CSS loading is expected to be more relevant and applicable to actual field problems.

C_r was used to quantify discrepancies in the liquefaction resistance between CTX and CSS tests. The results for C_r are summarized in Table 4, and Fig. 8 presents the C_r ratio, which is the ratio of the CRR required to cause liquefaction in 15 cycles under varying α in CSS tests (CRR_{15} in CSS) to that required for the same purpose and under the same conditions in the CTX tests (CRR_{15} in CTX). The graph shows the data obtained for σ'_{nc} (or σ'_{v0}) values of 100 and 200 kPa. Notably, the value of C_r is always smaller than 1 ($C_r < 1$). This is in agreement with the observation that a lower value of CRR_{15} is obtained from CSS tests compared with CTX tests. A smaller C_r ratio suggests a greater discrepancy in the liquefaction resistance between CTX and CSS tests. The C_r values are primarily dependent on D_r and α. For a given α, C_r for the loose state is invariably greater than that for the dense state. For instance, at $\alpha = 0$, regardless of σ'_{nc} (or σ'_{v0}), C_r is about 0.63 and

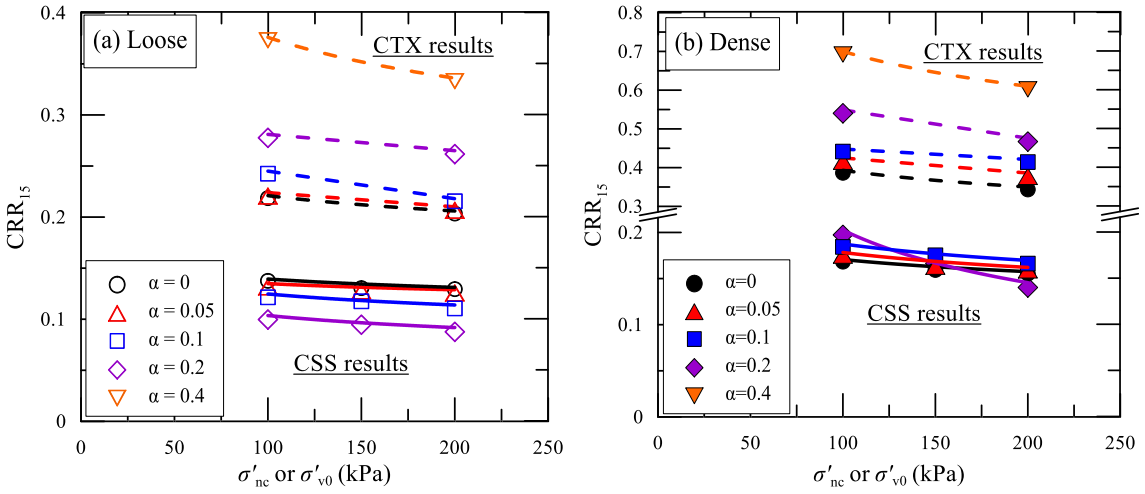

Fig. 7. Comparison of CRR_{15}–σ'_{nc} (or σ'_{v0}) curves measured in CTX and CSS tests.

Table 4
Results of reduction factor C_r on Nakdong River sand.

Sample	α	σ'_{v0} (kPa)	$C_r = (CRR_{15})_{CSS}/(CRR_{15})_{CTX}$	$\Delta C_r = (C_r)_{200} - (C_r)_{100}$	Average C_r
Loose (D_r = 40%)	0	100	0.633	0.008	0.637
		200	0.641		
	0.05	100	0.603	0.011	0.609
		200	0.614		
	0.1	100	0.506	0.012	0.512
		200	0.518		
	0.2	100	0.367	−0.024	0.355
		200	0.343		
Dense (D_r = 80%)	0	100	0.435	0.016	0.443
		200	0.451		
	0.05	100	0.421	0.001	0.422
		200	0.422		
	0.1	100	0.417	−0.016	0.409
		200	0.401		
	0.2	100	0.366	−0.063	0.335
		200	0.303		

Note: $(CRR_{15})_{CTX}$ and $(CRR_{15})_{CSS}$ are the cyclic resistance ratio required to cause liquefaction in 15 cycles under the cyclic triaxial and simple shear tests, respectively. $(C_r)_{100}$ and $(C_r)_{200}$ are the reduction factor C_r under the 100 and 200 kPa of σ'_{nc} (or σ'_{v0}), respectively.

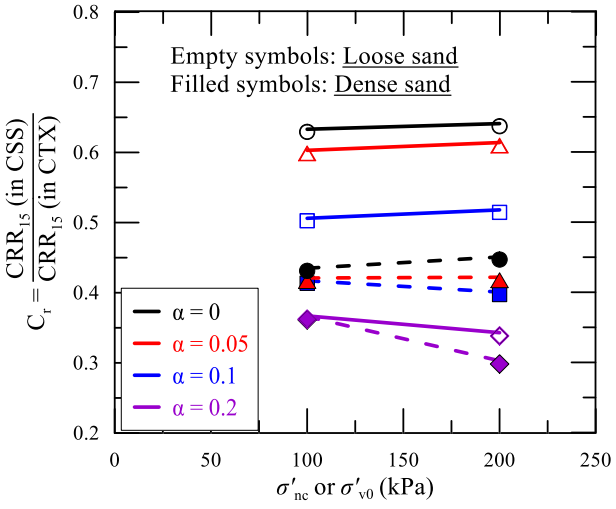

Fig. 8. Variation of C_r with σ'_{nc} (or σ'_{v0}) at different values of α.

about 0.43 for loose and dense sand, respectively. At a constant D_r, C_r decreases with increasing α. For example, at D_r = 40% and σ'_{nc} (or σ'_{v0}) = 100 kPa, C_r values decrease from 0.63 to 0.6 and from 0.5 to 0.37 when α increases from 0 to 0.05 and from 0.1 to 0.2, respectively. In other words, the overestimation of CRR_{15} in the CTX tests becomes more serious with an increase in the relative density or initial static shear stress. Compared with the small soil samples used in the CSS tests, the inherent anisotropy of large soil samples can result in a greater stiffness in the vertical direction (Sivathayalan and Ha 2011). This might have contributed to the increased resistance observed in the CTX tests. This initial anisotropy is generally altered by the anisotropy induced during the application of static shear (Wong and Arthur 1985). In this regard, an increase in the relative density or initial static shear stress is expected to enhance the effect of inherent anisotropy. This might explain the considerable shear strength increases observed in the CTX tests.

Fig. 9 shows the relationship between C_r and D_r for different values of α and σ'_{nc} (or σ'_{v0}). An interesting observation made from Table 4 and Fig. 9 is that C_r tended to show a small increase with an increase in σ'_{nc} (or σ'_{v0}) from 100 to 200 kPa when α was small, but it showed a slight decrease with an increase in σ'_{nc} (or σ'_{v0}) when α was large. Nonetheless, the difference of C_r is subtle. This behavior of C_r appears unlikely to contribute to features such as experimental errors or the influence of σ'_{nc} (or σ'_{v0}) and α, and further investigation is required to identify the reason for the behavior of C_r. Harder (1988) indicated that the value of C_r is dependent only on the relative density; however, Gokyer et al. (2019) observed an increase in C_r when the mean effective stress increased from 100 to 600 kPa for loose Ottawa sand (D_r = 40%). On the other hand, C_r

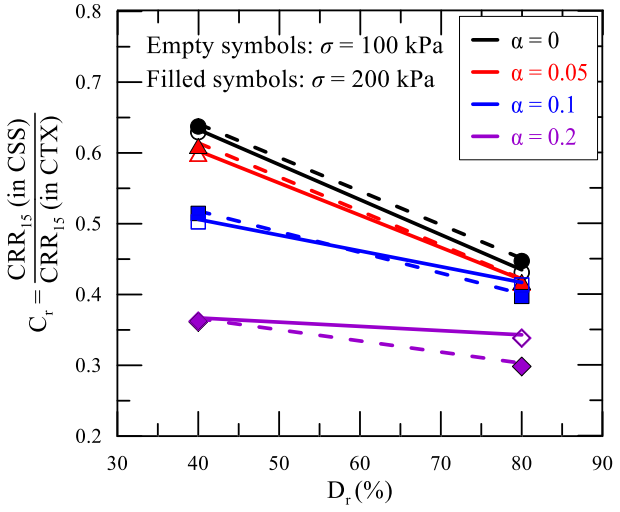

Fig. 9. Variation of C_r with D_r at different values of α.

was dependent on α for both loose and dense sand. For D_r = 40%, C_r decreased by approximately half (from ≈0.63 to ≈0.36) when α increased from 0 to 0.2. For D_r = 80%, a convergent C_r ratio ranging from 0.45 to 0.4 was observed when α increased from 0 to 0.1. It is also noteworthy that at α = 0.2, the value of C_r for loose sand was nearly equal to that for dense sand, namely 0.36. In practice, the cyclic resistance measured in CTX tests is converted into equivalent CSS values without considering the confining stress level, initial static shear level, or relative density state. A value of 0.6 is commonly adopted for the ratio C_r. If the C_r-data for Nakdong River sand shown in Fig. 9 are typical of other sands, the currently used value of C_r is suitable only for the loose sand for conditions where α is not considered or where α is small (≤0.05). For other stress conditions, the currently used high value of C_r could render the design too conservative. The use of C_r should depend on the relative density state and on the degree of initial static shear stress. On the basis of the results reported in Table 4, C_r-values of 0.637 and 0.443 are recommended for loose and dense sand when α is not considered, respectively. For α = 0.4, an average C_r value of 0.335 can be adopted for both loose and dense sand.

Fig. 10 presents the relationship between C_r and α for both loose and dense sand. Clearly, C_r decreases linearly with an increase in α, regardless of the σ'_{nc} (or σ'_{v0}) level. The sharp decrease in the C_r-ratio in loose sand especially indicates that the effect of α on C_r is more significant compared with the effect for dense sand. As loose sand has the highest potential for liquefaction, the effect of α on C_r should not be ignored in current engineering practice. For an increase in the α-value from 0 to 0.2, the linear relationship between C_r and α can be expressed as

$$C_r = -k_{(C_r-\alpha)}\alpha + b \quad (5)$$

where $k_{(C_r-\alpha)}$ represents the slope of the C_r–α curve and b is the C_r-value at α = 0. The values of $k_{(C_r-\alpha)}$ and b are dependent on the relative density and perhaps also the sand type.

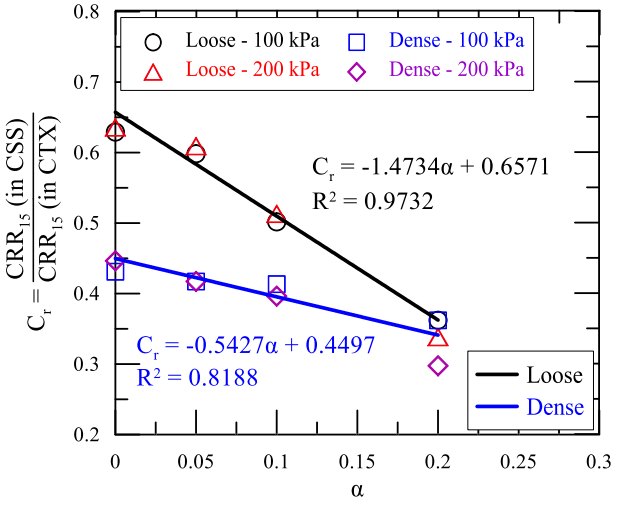

Fig. 10. Variation of C_r with α at different values of D_r.

In this study, $k_{(C_r-\alpha)}$ was 1.47 and 0.54 and b was 0.66 and 0.45 for loose and dense sand, respectively. Although the data are for limited relative densities for α varying from 0 to 0.2, the fairly high correlation coefficients are particularly noticeable, especially for loose sand.

3.2. Comparison of K_σ

The use of K_σ in routine liquefaction resistance evaluations of sand is especially important for high overburden stress states. K_σ has been defined as the CRR for any σ'_{nc} (or σ'_{v0}) to that at 100 kPa at a fixed D_r and α level ($K_\sigma = CRR_{\sigma,\alpha}/CRR_{100,\alpha}$). Fig. 11 presents a comparison of the variation of measured K_σ values with σ'_{nc} (or σ'_{v0}) between the CTX and CSS tests. A definite dependency of K_σ on σ'_{nc} (or σ'_{v0}) and D_r, in addition to that on α, is apparent from the data presented in Fig. 11(a)–(d). In both CTX and CSS tests, the K_σ decreased more rapidly when D_r increased from 40% to 80%. This result is consistent with the earlier findings of Vaid et al. (1985, 2001) and Vaid and Thomas (1995). The degree of decrease in K_σ with an increase in σ'_{nc} (or σ'_{v0}) up to 200 kPa in the CTX and CSS tests was essentially identical when α was not considered or less than 0.1. However, as soon as α increased to a high level (=0.2), the degree of decrease in K_σ in the CSS tests was more perceptible compared with that in the CTX tests, probably because of the different cyclic failure modes in the two types of tests. In the CSS tests, the use of α = 0.2 resulted in $\tau_{st} > \tau_{cyc}$, in which case no stress reversal occurred in the cyclic phase and cyclic failure was attributed to the plastic strain accumulation response. However, in the CTX tests, the use of α = 0.2 still caused partial cyclic stress reversal, and cyclic failure was attributed to the cyclic mobility response.

The effect of α on K_σ values is illustrated in Fig. 12. Regardless of the testing method, K_σ is not function of only σ'_{nc} (or σ'_{v0}), but it is also a function of α for both loose and dense sand. For loose sand, as shown in Fig. 12(a), the effect of α was not obvious until it increased to 0.1. For dense sand, as shown in Fig. 12(b), except for the case α = 0.2 in the CSS tests, the reduction in K_σ is not sensitive to the increase in α. K_σ-curves predicted using the NCEER-recommended method (Youd et al. 2001) and Boulanger method (Boulanger and Idriss 2004) are also plotted in Fig. 12. These methods are expected to work only if α is insignificant, since they do not consider the effect of α. Clearly, the Boulanger method yields higher K_σ-values than the NCEER-recommended method. A comparison of the Boulanger method's K_σ-values with the experimental K_σ-values shows that the Boulanger method is effective for predicting K_σ-curves for loose sand when α ≤ 0.05, but provides significantly lower K_σ-values for dense sand. On the other hand, the K_σ-values predicted using the NCEER-recommended method are always lower than the experimental K_σ-values for both loose and dense Nakdong River sand. Interestingly, the NCEER-

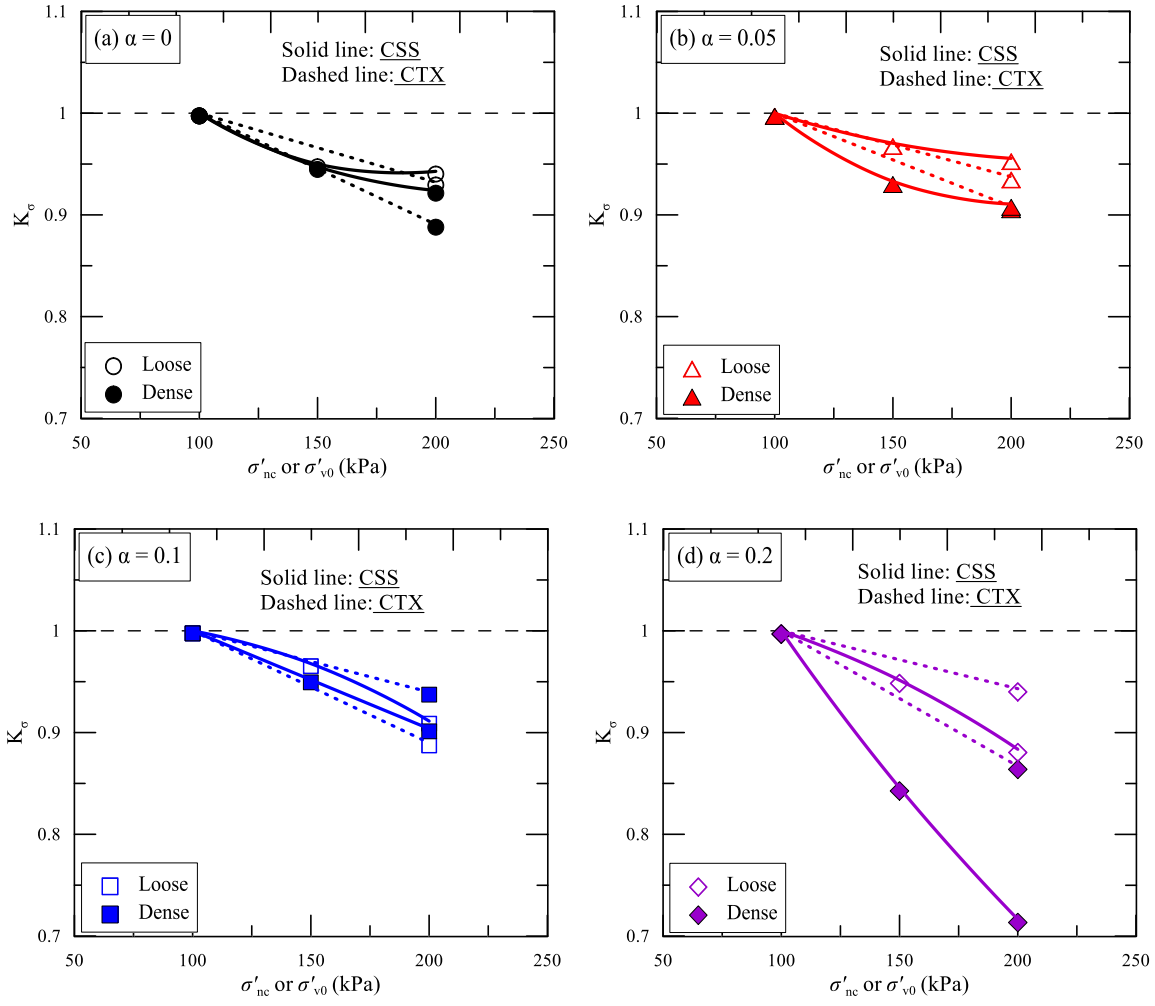

Fig. 11. Variation of K_σ with σ'_{nc} (or σ'_{v0}) at different values of α.

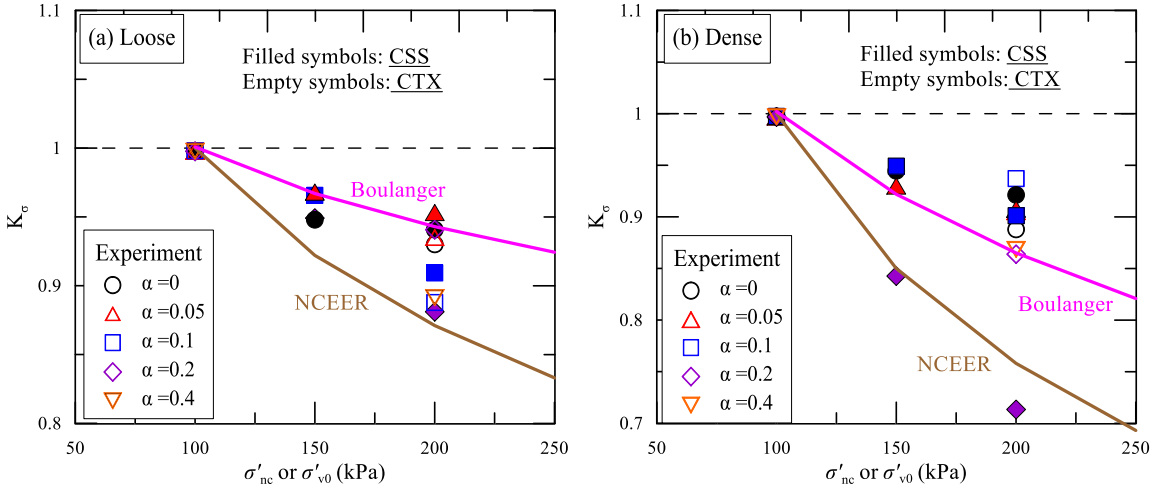

Fig. 12. Comparison of K_σ–σ'_{nc} (or σ'_{v0}) relationship with predictions by the NCEER-recommended and Boulanger methods.

recommended method appears to accurately capture the decreasing trend of K_σ with increasing σ'_{v0} at $D_r = 80\%$ and $\alpha = 0.2$ in the CSS tests. The effect of the confining stress on the reduction in cyclic resistance is much smaller than is currently considered in practice (Vaid and Sivathayalan 1996), and hence, the adoption of these lower values in the design based on some average relationship derived from the body of data presented by the NCEER-

recommended and Boulanger methods can result in conservative and costly designs.

3.3. Comparison of K_α

K_α is typically used to characterize the effect of the initial static shear stress, and it is defined as the ratio of the cyclic resistance at any static shear level to the cyclic resistance in the absence of static shear ($K_\alpha = CRR_{\sigma,\alpha}/CRR_{\sigma,0}$). A comparison of K_α obtained from the CTX and CSS tests is shown in Fig. 13. The K_α-values are plotted as a function of the normal (or vertical) effective stress, and the plots show the effect of α for both loose and dense Nakdong River sand. The test method clearly influences the K_α-results, regardless of the D_r and α levels. Overall, the K_α-values determined through the CTX tests are higher than those obtained in the CSS tests at comparable relative densities. For loose sand, regardless of the σ'_{nc} (or σ'_{v0}) level, the K_α-values determined through the CSS tests decrease continuously with an increase in the α-value, while those determined through the CTX tests increase continuously. For example, for α-values of 0.05, 0.1, and 0.2 at σ'_{nc} (or σ'_{v0}) = 100 kPa, the K_α-values were 0.964, 0.886, and 0.736, respectively, in the case of the CSS tests, and the K_α-values were 1.014, 1.109, 1.271, respectively, in the case of the CTX tests. Moreover, the K_α-values obtained by considering CSS conditions were 95%, 80%, and 58% of those obtained under the CTX conditions, respectively. For dense sand, the K_α-values determined through CTX tests increased continuously with an increase in α at σ'_{nc} = 100 and 200 kPa. However, the K_α-values determined through CSS tests for dense sand were dependent on the vertical effective stress. At σ'_{v0} = 100 kPa, K_α increased continuously with increasing α. At σ'_{v0} = 150 and 200 kPa, K_α increased with an increase in α up to a value of 0.1. Above this value, K_α shows a slight decrease when α continued to increase to 0.2. For α-values of 0.05, 0.1, and 0.2 for dense sand, at σ'_{nc} (or σ'_{v0}) = 100 kPa, K_α-values obtained by considering CSS conditions were 97%, 96%, and 85% of those obtained under CTX conditions, respectively; at σ'_{nc} (or σ'_{v0}) = 200 kPa, these ratios were 94%, 89%, and 67%, respectively.

Superimposed on Fig. 13 are the predicted K_α-zones determined from the Harder and Boulanger (1997) method. In Fig. 13(a), the experimental K_α-trends reconstructed from CSS tests fall in the $D_r \approx 35\%$ zone of the Harder and Boulanger method. However, those reconstructed from CTX tests fall in the $D_r \approx 50\%$–70% zone, despite all tests having been performed on sand with a relative density of 40%. A similar conclusion was reported by Vaid et al. (2001). These researchers noted that the empirical correction factors of Harder and Boulanger (1997) grossly underestimated the actual cyclic resistance of Fraser River sand with a relative density of 40% obtained from CTX tests; the observed K_α was greater than 1 while the estimated value was less than 1 when α varied up to 0.4. On the other hand, as shown in Fig. 13(b), the experimental K_α-trends in both the CTX and CSS tests for a relative density of 80% mainly fell in the $D_r \approx 50\%$–70% zone of the Harder and Boulanger method.

A parabolic function expressed the relationship between K_α and α well for both the CTX and CSS tests, as shown in Fig. 14. For loose sand, the K_α-α data could be fitted by specific parabolic functions, depending on the test method and regardless of σ'_{nc} (or σ'_{v0}). For dense sand, the parabolic functions depended on the test method and value of σ'_{nc} (or σ'_{v0}). The specific expressions of K_α–α functions based on the test method, D_r, and σ'_{nc} (or σ'_{v0}) are presented in Fig. 14(a) and (b). A general expression for K_α can be written as

$$K_\alpha = a_1\alpha^2 + a_2\alpha + 1 \quad (6)$$

The difference in K_α-values between the CTX and CSS tests ($\Delta K_\alpha = (K_\alpha)_{CTX} - (K_\alpha)_{CSS}$) is shown in Fig. 15. The ΔK_α–α trend was also well expressed by a parabolic correlation. For loose sand, the relationship between ΔK_α and α was independent of σ'_{nc} (or σ'_{v0}), and it could be

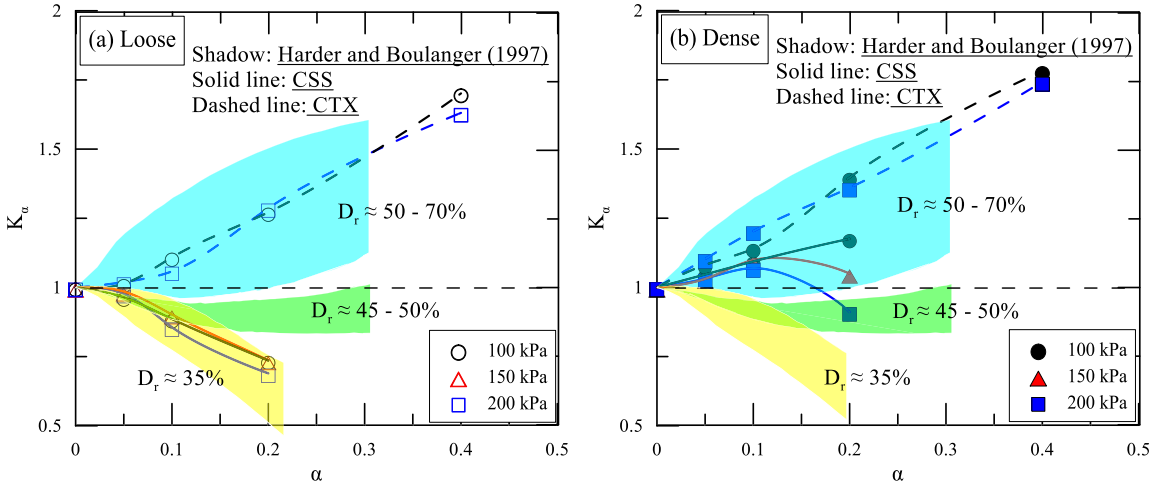

Fig. 13. Comparison of K_α–α relationship in CTX and CSS tests.

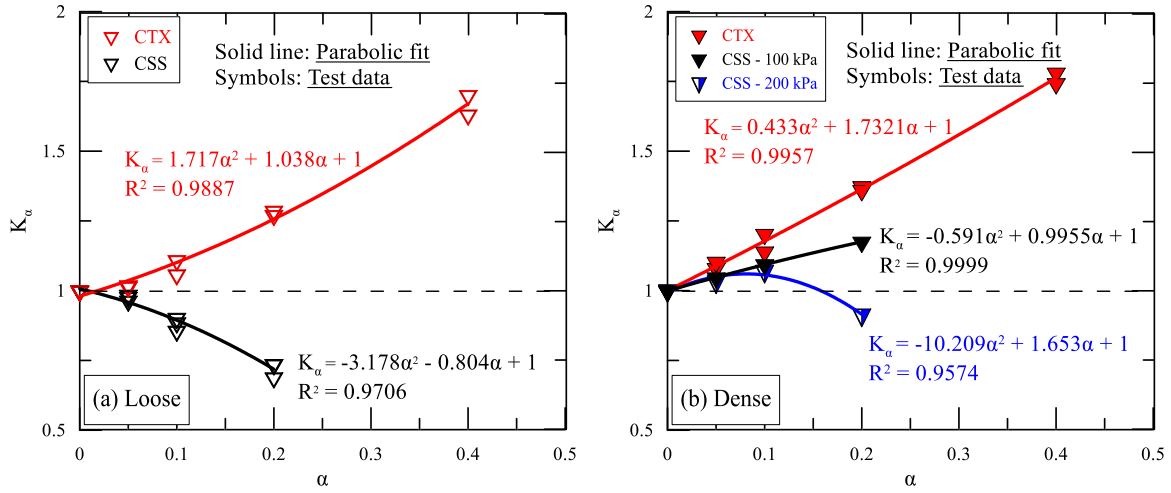

Fig. 14. Parabolic function for K_α–α relationship in CTX and CSS tests.

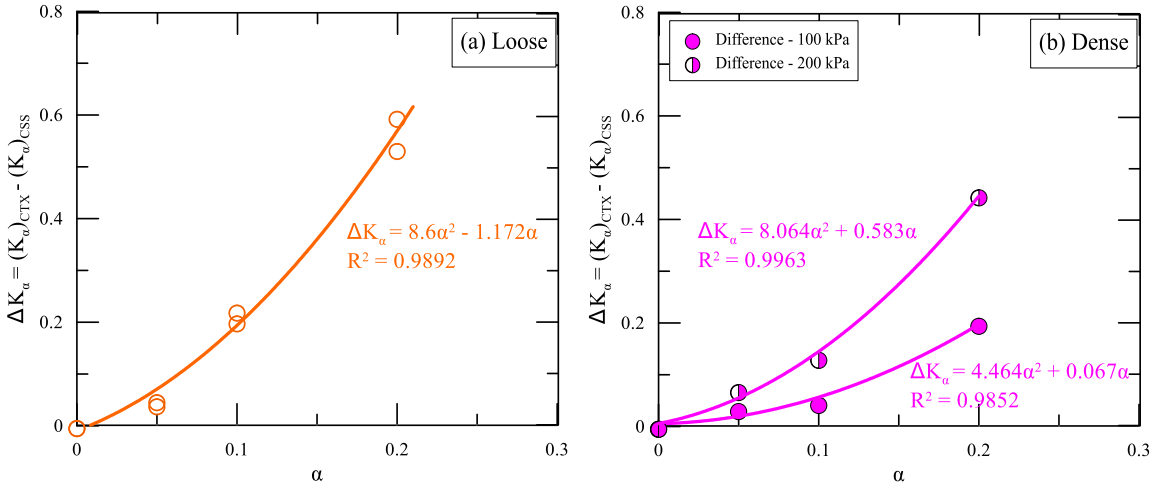

Fig. 15. The difference of K_α varied with α in CTX and CSS tests.

expressed by a unique expression as shown in Fig. 15(a). For dense sand, as shown in Fig. 15(b), the expressions for the ΔK_α–α relationship depended on the σ'_{nc} (or σ'_{v0}) level. A general expression for ΔK_α can be written as

$$\Delta K_\alpha = b_1\alpha^2 + b_2\alpha \tag{7}$$

Here, the parameters a_1, a_2, b_1, andb_2 change with the test method, relative density, normal (or vertical) effective stress, and perhaps also with the sand type. These correlations can be used to convert K_α-values obtained in the CTX test to those appropriate for the CSS test and vice versa.

The relationship between the liquefaction resistance in the CTX test and that in the CSS test appears to be a function of the apparatus used, sample preparation method, relative density, confining stress, initial static shear stress, and probably other factors. This makes it difficult to establish a specific strength curve above which liquefaction occurs (Bhatia et al. 1985). Cetin and Bilge (2013, 2014) indicated that D_r, τ_{st}, τ_{cyc}, and the shear stress reversal and strain levels are the main parameters that determine the cyclic resistance of cohesionless soils. They suggested using a collectively dependent set of correction schemes, which requires a performance-based assessment of liquefaction with an iterative convergence scheme. In this study, we attempted to develop general formulations for C_r, K_α, and ΔK_α as functions of α by considering the effects of D_r and σ'_{nc} (or σ'_{v0}) on the basis of experimental data. Trial empirical methods are presented here for facilitating the acquisition of more knowledge and as a basis for future works. These can serve as a good starting point for the quantitative analysis of correlative liquefaction resistances measured in CTX and CSS tests when more relevant data are available by using, the same approach used in the present research.

4. Conclusions

This paper presents a study in which the liquefaction resistance and correction factors K_σ and K_α measured under CTX conditions were compared with those obtained under CSS conditions. The comparisons were performed

by considering a single type of sand to minimize the number of influencing factors; moreover, we used similar methods of sample preparation, considered similar relative densities and stress states, used apparatuses manufactured by one company, and assigned all testing to a single operator. The following conclusions were drawn.

1. The sand liquefaction resistance obtained from CTX tests was always greater than that acquired from CSS tests. The value of C_r decreased with an increase in D_r and/or α; however, C_r was not significantly affected by σ'_{nc} (σ'_{v0}). For $D_r = 40\%$ and $\alpha = 0$, C_r was about 0.63, but for $D_r = 80\%$ and $\alpha = 0.4$, C_r decreased to about 0.36. These results imply that the difference in the liquefaction resistance between the CTX and CSS tests increase for denser states and/or higher initial static shear stress.
2. K_σ in the CTX and CSS tests was essentially identical when α increased up to a value of 0.1. Furthermore, the Boulanger method is effective in predicting K_σ-trends for loose sand for $\alpha \leq 0.05$, but predicts lower K_σ for dense sand. The predictions of the NCEER-recommended method are always lower than the experimental K_σ-values for both loose and dense sand.
3. K_α obtained through CSS tests is always lower than that acquired through CTX tests. The K_α-values obtained through CSS tests are 97%–58% of those observed in CTX tests, and the K_α-values depend on the combination of D_r, σ'_{nc} (σ'_{v0}), and α. Compared with experimental K_α values obtained through CTX tests, those acquired through CSS tests accord better with the predictions of the Harder and Boulanger method.
4. The relationship between K_α and α in both the CTX and CSS tests can be fitted well by a specific parabolic function. Furthermore, the difference between the K_α-values of the CTX and CSS tests can be expressed as a parabolic correlation involving α. These correlations can be used to convert K_α-values obtained in the CTX test to those appropriate for the CSS test and vice versa.

Acknowledgements

This work was supported by the National Research Foundation of Korea (NRF) grant funded by the Korean government (MSIT) (No. NRF-2018R1A5A1025137).

References

Bhatia, S.K., Schwab, J., Ishibashi, I., 1985. Cyclic simple shear, torsional shear and triaxial–A comparative study. Book. Advances in the Art of Testing Soils under Cyclic Conditions, pp. 232–254.

Bjerrum, L., Landva, A., 1966. Direct simple shear tests on a Norwegian quick clay. Geotechnique 16 (1), 1–20.

Boulanger, R.W., 2003. High overburden stress effects in liquefaction analyses. J. Geotech. Geoenviron. Eng. ASCE 129 (12), 1071–1082.

Boulanger, R.W., Idriss, I.M., 2004. State normalization of penetration resistances and the effect of overburden stress on liquefaction resistance. Proceedings, 11th International Conference on Soil Dynamics and Earthquake Engineering and 3rd International Conference on Earthquake Geotechnical Engineering, (Ed.) Doolin et al., 2, 484–491. Stallion Press.

Cetin, K.O., Bilge, H.T., 2013. Stress scaling factors for seismic soil liquefaction engineering problems: a performance-based approach. Proceedings, International Conference on Earthquake Geotechnical Engineering from Case History to Practice in Honor of Prof. Kenji Ishihara.

Cetin, K.O., Bilge, H.T., 2014. Unified assessment of stress scaling factors for liquefaction engineering problems. Proceedings, Geo-Congress 2014 Technical Papers, 4293–4302.

Fonseca, A.V.D., Soares, M., Fourie, A.B., 2015. Cyclic DSS tests for the evaluation of stress densification effects in liquefaction assessment. Soil Dyn. Earthq. Eng. 75, 98–111.

Gokyer, K., Zehtab, K., Marr, W.A., Werden, S.K., Apostolov, A., 2019. Cyclic response of Ottawa sand under different test conditions: Cyclic triaxial, unidirectional and bidirectional direct simple shear. Proceedings, 7th International Conference on Earthquake Geotechnical Engineering, pp. 2674–2681.

Haeri, S.M., Pouragha, M., 2010. An insight to the effect of initial static shear stress on the liquefaction of sands. Proceedings, 15th International Conference on Recent Advances in Geotechnical Earthquake Engineering and Soil Dynamics, Paper No. 1.08b.

Harder Jr., L.F., 1988. Use of penetration tests to determine the cyclic load resistance of gravelly soils. University of California, Berkeley.

Harder, L.F., Jr., Boulanger, R.W., 1997. Application of Kα and Kα correction factors. Paper No. 167-190. Proceedings, the NCEER workshop on evaluation of liquefaction resistance of soils, National Center for Earthquake Engineering Research, State University of New York at Buffalo.

Hoque, M.M., 2016. Evaluation of dynamic properties of a sandy soil using cyclic triaxial test. Bangladesh University of Engineering and Technology, Thesis.

Hosono, Y. and Yoshimine, M. (2004). Liquefaction of sand in simple shear Condition. In Cyclic Behavior of Soils and Liquefaction Phenomena, Triantafyllidis (Ed.), 129–136. London: Taylor & Francis Group.

Ishihara, K., 1996. Soil behaviour in earthquake Geotechnics. Clarendon Press, Oxford.

Jis, A., 2009. Test method for minimum and maximum densities of sands. Japan. Geotech. Soc. 1224.

Ladd, R.S., 1978. Preparing test specimens using under compaction. J. Geotech. Testing 1 (1), 16–23.

Liu, A.H., Stewart, J.P., Abrahamson, N.A., Moriwaki, Y., 2001. Equivalent number of uniform stress cycles for soil liquefaction analysis. J. Geotech. Geoenviron. Eng. 127 (12), 1017–1026.

Marcuson, W.F.III., Krinitzsky, E.L., 1976. Dynamic analysis of Fort Peck Dam. Technical Report S-76-1, U. S. Army Engineering Waterways Experiment Station.

NRC, 1985. Liquefaction of soils during earthquake. National Research Council. National Academic Press, Washington, D. C. Report No. CETS–EE–001.

Park, S.S., Nong, Z.Z., Lee, D.E., 2020. Effect of vertical effective and initial static shear stresses on the liquefaction resistance of sands in cyclic direct simple shear tests. Soils Found. https://doi.org/10.1016/j.sandf.2020.09.007.

Peacock, W.H., Seed, H.B., 1968. Sand liquefaction under cyclic loading simple shear conditions. J. Soil Mech. Found. Divis., ASCE 94 (SM3), 689–708.

Pillai, V.S., Stewart, R.A., 1994. Evaluation of liquefaction potential of foundation soils at Duncan dam. Can. Geotech. J. 31, 951–966.

Seed, R.B., Harder Jr., L.F., 1990. SPT-based analysis of cyclic pore pressure generation and undrained residual strength. Proceedings, the H. Bolton Seed Memorial Symposium. BiTech Publishers, Vancouver, pp. 351–376.

Seed, H.B., Idriss, I.M., 1981. Evaluation of liquefaction potential of sand deposits based on observations of performance in previous earthquakes. Session on in situ testing to evaluate liquefaction susceptibility,

ASCE, National Convention, State Louis, Missouri, USA, Pre-print, 81–544.

Seed, H.B., Idriss, I.M., Makdisi, F., Banerjee, N., 1975. Representation of irregular stress time histories by equivalent uniform stress series in liquefaction analysis. University of California Berkeley, California, Earthquake Engineering Research Centre.

Silver, M.L., Tatsuoka, F., Phukunhaphan, A., Avramidis, A.S., 1980. Cyclic undrained strength of sand by triaxial test and simple shear test. Proceedings, 7th World Conference on Earthquake Engineering, 3, 281–288.

Sivathayalan, S., Ha, D., 2011. Effect of static shear stress on the cyclic resistance of sands in simple shear loading. Can. Geotech. J. 48, 1471–1484.

Sze, H.Y., 2010. Initial shear and confining stress effects on cyclic behavior and liquefaction resistance of sands Ph.D. Thesis. Hong Kong University, Hong Kong.

Tatsuoka, F., Muramatsu, M., Sasaki, T., 1982. Cyclic undrained stress-strain behavior of dense sands by torsional simple shear test. Soils Found. 23 (1), 47–60.

Toki, S., Tatsuoka, F., Miura, S., Yoshimi, Y., Yasuda, S., Makihara, Y., 1986. Cyclic undrained triaxial strength of sand by a cooperative test program. Soils Found. 26 (3), 117–128.

Vaid, Y.P., Chern, J.C., 1985. Cyclic and monotonic undrained response of sands. In: Advances in the art of testing soils under cyclic loading conditions, Detroit, Mich., Edited by V. Khosla. ASCE, New York, 120–147.

Vaid, Y.P., Sivathayalan, S., 1996. Static and cyclic liquefaction potential of Fraser Delta sand in simple shear and triaxial tests. Can. Geotech. J. 33 (2), 281–289.

Vaid, Y.P., Thomas, J., 1995. Liquefaction and post liquefaction behavior of sand. J. Geotech. Eng., ASCE 121 (2), 163–173.

Vaid, Y.P., Chern, J.C., Tumi, H., 1985. Confining pressure, grain angularity, and liquefaction. J. Geotech. Eng., ASCE 111 (10), 1229–1235.

Vaid, Y.P., Stedman, J.D., Sivathayalan, S., 2001. Confining stress and static shear effects in cyclic liquefaction. Can. Geotech. J. 38, 580–591.

Wei, X., Yang, J., 2015. The effects of initial static shear stress on liquefaction resistance of silty sand. Proceedings, 6th International Conference on Earthquake Geotechnical Engineering, Christchurch, New Zealand.

Wijewickreme, D., Sriskandakumar, S., Byrne, P., 2005. Cyclic loading response of loose air-pluviated Fraser River sand for validation of numerical models simulating centrifuge tests. Can. Geotech. J. 42, 550–561.

Wong, R.K.S., Arthur, J.R.F., 1985. Induce and inherent anisotropy in sand. Geotechnique 35 (4), 471–481.

Yang, J., Sze, H.Y., 2011a. Cyclic strength of sand under sustained shear stress. J. Geotech. Geoenviron. Eng. 137 (12), 1275–1285.

Yang, J., Sze, H.Y., 2011b. Cyclic behavior and resistance of saturated sand under non-symmetrical loading conditions. Geotechnique 61 (1), 59–73.

Youd, T.L., Idriss, I.M., Andrus, R.D., et al., 2001. Liquefaction Resistance of Soils: Summary Report from the 1996 NCEER and 1998 NCEER/NSF Workshops on Evaluation of Liquefaction Resistance of Soils. J. Geotech. Geoenviron. Eng. 127 (10), 817–833.

Zhang, L., Evans, T.M., 2018. Boundary effects in discrete element method modeling of undrained cyclic triaxial and simple shear elements tests. Granular Matter 20.